Physics Letters B 733 (2014) 52–57

Contents lists available at ScienceDirect

Physics Letters B

www.elsevier.com/locate/physletb

Collectivity in A ∼ 70 nuclei studied via lifetime measurements in ^{70}Br and ^{68,70}Se

A.J. Nichols [a,*], R. Wadsworth [a], H. Iwasaki [b], K. Kaneko [c], A. Lemasson [b,d], G. de Angelis [e], V.M. Bader [b], T. Baugher [b], D. Bazin [b], M.A. Bentley [a], J.S. Berryman [b], T. Braunroth [f], P.J. Davies [a], A. Dewald [f], C. Fransen [f], A. Gade [b], M. Hackstein [f], J. Henderson [a], D.G. Jenkins [a], D. Miller [g], C. Morse [b], I. Paterson [a], E.C. Simpson [a], S.R. Stroberg [b], D. Weisshaar [b], K. Whitmore [b], K. Wimmer [b]

[a] Department of Physics, University of York, Heslington, York YO10 5DD, UK
[b] National Superconducting Cyclotron Laboratory and Department of Physics and Astronomy, Michigan State University, 164 S. Shaw Lane, East Lansing, MI 48825-1321, USA
[c] Department of Physics, Kyushu Sangyo University, Fukuoka 813-8503, Japan
[d] Grand Accélérateur National d'Ions Lourds, Bd. Henri Becquerel, BP 55027, F-14076 Caen Cedex 05, France
[e] Laboratori Nazionali di Legnaro dell'INFN, Legnaro (Padova) I-35020, Italy
[f] Institut für Kernphysik der Universität zu Köln, Köln 50937, Germany
[g] Department of Physics and Astronomy, University of Tennessee, Knoxville, TN 37996, USA

ARTICLE INFO

Article history:
Received 31 January 2014
Received in revised form 8 April 2014
Accepted 9 April 2014
Available online 15 April 2014
Editor: V. Metag

Keywords:
Nuclear transition probabilities
Nucleon knockout reactions
Lifetimes

ABSTRACT

Transition strengths for decays from low-lying states in A ∼ 70 nuclei have been deduced from lifetime measurements using the recoil distance Doppler shift technique. The results confirm the collectivity previously reported for the $2_1^+ \rightarrow 0_{gs}^+$ decay in ^{68}Se and reveal a relative decrease in collectivity in ^{70}Br. This trend is reproduced by shell model calculations using the GXPF1A interaction in an *fp* model space including the Coulomb, spin-orbit and isospin non-conserving interactions. The $3_1^+ \rightarrow 2_1^+$ decay in ^{70}Br is found to have a very small B(M1) value, which is consistent with the configuration of the state being dominated by the coupling of $f_{\frac{5}{2}}$ protons and neutrons. The results suggest that the $g_{\frac{9}{2}}$ orbit does not play an important role at low spin in these nuclei. The B(E2) values for the decays of the (T = 1) 2_1^+ states in ^{70}Br and ^{70}Se are almost identical, suggesting there is no major shape change between the two nuclei at low spin.

In N = Z nuclei, neutron and proton shell effects can act coherently due to both nucleons occupying the same orbitals. This in turn promotes a greater sensitivity of nuclear properties, such as deformation-driving effects resulting from proton–neutron correlations [1], to small changes in nucleon number. The A ∼ 70, N = Z region of the nuclide chart, where valence nucleons may occupy the *fpg*-shell, is of interest due to the deformation-driving effects of the $g_{\frac{9}{2}}$ intruder orbital [2,3] and its role in increasing collectivity as the mid-shell point, located between the nucleon numbers of 28 and 50, is approached. This mid-shell region is of added interest because it is also the location where nuclear shapes vary rapidly with both nucleon number and angular momentum (e.g., see [4]). These effects arise due to the presence of large sub-shell gaps at nucleon numbers of 34 and 36 (oblate), 34 and 38 (prolate) and 40 (spherical) [3,5]. In addition, nuclei in this region have competing, low-lying configurations resulting from more than one shape, which results in the rapid shape changes with angular momentum. These features make this region very challenging from a theoretical perspective.

Reduced transition strengths can yield information on quadrupole collectivity and nuclear deformation as well as providing a sensitive test of nuclear models. Electromagnetic transition strengths (B(E2) values) between the first excited 2^+ state and the ground state have previously been measured for several even–even N = Z nuclei in the region: ^{64}Ge [6], ^{68}Se [7], ^{72}Kr [8] and most recently ^{76}Sr [9]. These results suggest a rapid increase in B(E2) values, and hence deformation, between ^{68}Se (B(E2↓) = 432(58) e^2 fm^4) [7] and ^{72}Kr (B(E2↓) = 999(129) e^2 fm^4) [8]. There are currently no transition strength data for any of the

* Corresponding author.
E-mail address: an527@york.ac.uk (A.J. Nichols).

http://dx.doi.org/10.1016/j.physletb.2014.04.016

Table 1
Initial and final level spins/parities, γ-ray energies, extracted transition intensities (I_γ), measured mean state lifetimes (τ_m) and corresponding reduced transition strengths (B(ML↓)) studied in this work. The table contains both present results (Pres.) and previously published results (Lit.). All γ-ray intensities are normalised relative to the $2_1^+ \rightarrow 0_{gs}^+$ intensity for each nucleus. For some feeding states to the yrast 2^+ states, measured effective lifetimes τ_m^{eff} are shown. B(E2↓) values are given in units of $e^2\,fm^4$ and B(M1↓) in units of μ_N^2. The errors quoted include both statistical and systematic effects.

	J_i^π	J_f^π	E_γ [keV]	Mult.	I_γ [%]	τ_m^{eff} [ps]	τ_m [ps]		B(λL↓)	
							Pres.	Lit.	Pres.	Lit.
^{70}Br	5_1^+	3_1^+	321	E2	11.9(17)	–	540(120)	–	450(100)	–
	3_1^+	2_1^+	403	M1	23.6(26)	–	32(15)	–	0.027(12)	–
	2_1^+	0_{gs}^+	934	E2	100	–	3.96(58)	–	291(43)	–
^{70}Se	4_1^+	2_1^+	1093	E2	30.5(16)	4.38(37)	–	1.4(1)[a]	–	560(40)[a]
	$3_1^{(-)}$	2_1^+	1574	E1	16.5(13)	1.86(57)	–	6.1(9)[b]	–	–
	2_2^+	2_1^+	655	M1/E2	7.1(10)	6.73(74)	–	4.8(13)[b]	–	–
	2_1^+	0_{gs}^+	945	E2	100	–	3.28(37)	3.2(2)[a]	332(37)	342(19)[a]
^{68}Se	4_1^+	2_1^+	1088	E2	48(10)	–	–	–	–	–
	2_1^+	0_{gs}^+	854	E2	100	–	4.60(82)	4.2(6)[c]	392(70)	432(58)[c]

[a] From [13].
[b] From [21].
[c] From [7].

odd–odd N = Z nuclei in this region, preventing comparison with calculations that include such nuclei [2,10]. The present work focuses on the self-conjugate nucleus ^{70}Br, which resides between ^{68}Se and ^{72}Kr, in order to define the location along the N = Z line where collectivity starts to rapidly increase.

A further interest in A ∼ 70, N ∼ Z nuclei results from indications [11,12] that small electromagnetic shifts of single-proton levels can yield different shape-driving effects, potentially resulting in different shapes across an isobaric multiplet, which in turn would result in a significant breakdown of isospin symmetry. It has been suggested that this may be the origin of the observed negative Coulomb energy difference between ^{70}Se and ^{70}Br [11]. It is of interest therefore to compare transition strengths from decays of isobaric analogue states in these two nuclei.

In this letter, we report on a measurement of the lifetimes of the first (T = 1) 2^+ states in ^{70}Br and ^{70}Se. Also reported are the lifetimes of the yrast 3^+ and 5^+ T = 0 states in ^{70}Br and the first (T = 0) 2^+ state in ^{68}Se. The ^{70}Br results provide the first lifetime data in an odd–odd N = Z nucleus above ^{54}Co. Previous work on ^{68}Se, using relativistic Coulomb excitation techniques, established a B(E2↑) value for the $0_{gs}^+ \rightarrow 2_1^+$ transition [7], whilst for ^{70}Se a B(E2↓) value was obtained using a recoil distance method to measure the lifetime of the yrast 2^+ state [13].

The present experiment was performed at the National Superconducting Cyclotron Laboratory (NSCL) at Michigan State University, USA. The Coupled Cyclotron Facility [14] produced a ^{78}Kr primary beam at 150 MeV/u. This beam was used to bombard a primary production target of 399 mg/cm^2 ^{9}Be and produce the radioactive secondary beams of interest, ^{71}Br and ^{70}Se, via projectile fragmentation. These secondary beams were selected using the A1900 fragment separator [15]. The ^{71}Br and ^{70}Se beams had typical intensities (purities) of 1.5×10^5 pps (8%) and 7.1×10^5 pps (38%), respectively.

The present experiment utilised the ^{9}Be(^{71}Br, ^{70}Br + γ), ^{9}Be(^{70}Se, ^{68}Se + γ) and ^{9}Be(^{70}Se, ^{70}Se + γ) reactions to study the low-lying excited states in ^{70}Br, ^{68}Se and ^{70}Se, respectively. To facilitate these reactions, the secondary beams were impinged on a 96 mg/cm^2 ^{9}Be target foil housed in a plunger device at the target position of the S800 spectrograph [16]. The TRIple PLunger for EXotic beams (TRIPLEX), developed by the Köln-NSCL collaboration [17], was utilised in this work. This plunger is designed to house up to three target or degrader foils. In this experiment only a single target and one Ta degrader foil of 403 mg/cm^2 were used. The third position housed a thin polypropylene foil, which was used to strip outgoing recoils of any remaining atomic electrons. The plunger device was used to measure the lifetimes of excited states using the recoil distance Doppler shift (RDDS) technique [18]. Data were taken for four target-degrader separations (275 μm, 323 μm, 425 μm and 4.275 mm). The three smallest separations allowed for the analysis of lifetimes in the picosecond range, whereas the large target-degrader separation (4.275 mm) was used to measure contributions arising from reactions and excitations of recoils in the degrader foil.

The four quoted target-degrader separations were obtained from a distance calibration. This calibration is typically performed using a capacitance technique [18]. From this calibration it was possible to obtain accurate knowledge of the relative distances between the foils. An offset was then deduced to translate these relative distances into absolute target-degrader separations. Due to complications caused by the distortion of the foils at the edges during mounting, the offset was not deduced by the capacitance technique, but instead by calibrating to a known lifetime in the literature. The lifetime of the first 2^+ state in ^{62}Zn, with a literature result of 4.2(2) ps based on a weighted average of several studies [19], was used as this nucleus was populated strongly in the data from the ^{70}Se secondary beam. Using this result the foil separation offset was deduced to be 275(30) μm, and from this the absolute separation distances were extracted. This offset was then used to perform a separate analysis of the lifetime of the first 2^+ state in ^{70}Se, which had been measured previously [13]. The value obtained agrees with the published value (see Table 1) and is discussed in more detail below.

De-excitation γ-rays from the recoiling reaction products were detected using SeGA [20], an array of fifteen segmented high-purity germanium detectors that surrounded the plunger target position. In the present experiment, 7(8) of these detectors were placed at 30° (140°) to the beam direction. Secondary beam isotones transmitted through the A1900 separator were cleanly separated from each other via their time-of-flight between two plastic scintillators placed before the secondary target position. The reaction products left the degrader foil with velocities of approximately 0.3c and were subsequently bent into the focal plane of the S800 spectrograph [16], where they were detected and identified on an event-by-event basis from energy-loss and time-of-flight information using a compartmentalised ion chamber and plastic scintillators, respectively. This identification provided very good recoil separation and allowed for clean software cuts on individual reaction products.

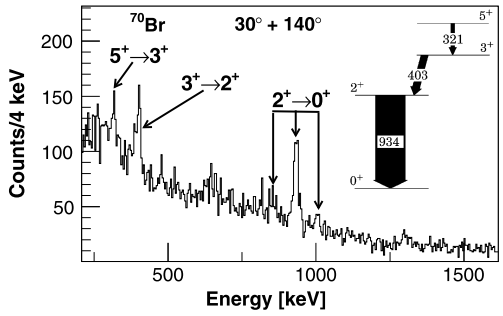

Fig. 1. Experimental γ spectrum from both SeGA rings gated on ^{70}Br recoils at a target-degrader separation of 275 μm, identifying the observed transitions. Inset: level scheme showing the population of states in ^{70}Br in this work and the associated decay γ-rays. Energies are given in keV. Arrow thicknesses correspond to the intensity of the transition relative to the $2^+_1 \rightarrow 0^+_{gs}$ transition.

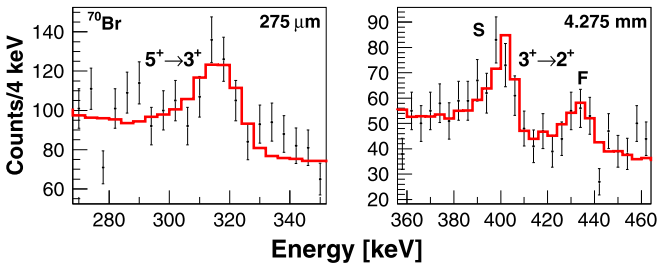

Fig. 2. (Colour online.) Data (black points) and best-fit simulated lineshapes (red line) for the 321 keV $5^+_1 \rightarrow 3^+_1$ transition (left) and the 403 keV $3^+_1 \rightarrow 2^+_1$ transition (right) in ^{70}Br. Both spectra are for 30° detectors. The 5^+_1 state has a long lifetime, therefore a lineshape method was used (see [9]). The lifetime of the 3^+_1 state could only be deduced via the RDDS method from the 4.275 mm data. Fast (F) and slow (S) components for the $3^+_1 \rightarrow 2^+_1$ transition are labelled and correspond to decays before and after the degrader foil, respectively.

Data were taken with a single target foil in the plunger to identify the γ-ray feeding of the states of interest. A level scheme showing the observed γ-rays in ^{70}Br is shown in the inset to Fig. 1 and the intensities are listed in Table 1. Fig. 1 shows data taken for both SeGA rings at a target-degrader separation of 275 μm and identifies the observed γ transitions in ^{70}Br. The 2^+_1 state in ^{68}Se was fed by the 4^+_1 state with an intensity of 48(10)%. In ^{70}Se, three feeding transitions to the yrast 2^+ state were observed: the $4^+_1 \rightarrow 2^+_1$ transition, feeding with an intensity of 30.5(16)%; the $2^+_2 \rightarrow 2^+_1$ transition, with an intensity of 7.1(10)%; and the $3^{(-)}_1 \rightarrow 2^+_1$ transition, with an intensity of 16.5(13)% – see Table 1. Any additional γ-ray intensity after considering all observable feeding states was assumed to result from direct (fast) population of the state.

Lifetimes were extracted by comparing the experimental γ-ray spectra to simulations. A background was added to the simulations to accurately replicate the experimental background in the region of lifetime sensitivity. In all cases a linear background was found to be sufficient. Fits were made separately to the forward (30°) and backward (140°) SeGA rings using a χ^2 minimisation. Simulations were generated using a dedicated lifetime code developed at NSCL [9] which utilises the GEANT4 framework [22]. The use of these simulations has been studied in detail and is presented in Ref. [23]. The simulations can be tailored to accurately replicate the experimental set-up by empirically fitting simulated particle spectra to their experimental equivalents. The simulation package allows for accurate consideration of complex feeding histories, with each feeding state having an independent lifetime and feeding intensity. Simulated γ-ray spectra with varying lifetimes are then compared with experimental data.

Lifetimes of all the observed states feeding the yrast 2^+ states in this work were measured and incorporated into the simulations. The two exceptions to this are the 2^+_2 state in ^{62}Zn and the 4^+_1 state in ^{68}Se, whose lifetimes could not be measured due to poor statistics. In the case of the ^{62}Zn 2^+_2 state, the literature lifetime was assumed. In the case of the ^{68}Se 4^+_1 state, no literature lifetime has been previously measured and so a short lifetime was assumed. In ^{70}Br, the 5^+_1 state lifetime was measured using a lineshape method with forward angle data as described in Ref. [9], since it was too long-lived for the RDDS technique to be employed. The spectra at target-degrader separations of 275 μm and 323 μm provided the cleanest data for the 321 keV γ-ray analysis. The weighted mean lifetime extracted from these two data sets is 540(120) ps. Fig. 2 shows an example best lineshape fit for one data set. Since no higher-lying states were observed feeding the 5^+_1 state, this result is assumed to represent the actual lifetime of the state. The measured lifetime gives a corresponding B(E2;$5^+_1 \rightarrow 3^+_1$) of 450(100) e^2 fm^4. The 403 keV γ-ray from the 3^+_1 state was observed to only contain fast (F) and slow (S) components at the largest distance measured (4.275 mm) – see Fig. 2. The weighted mean lifetime from the fits of the 30° and 140° spectra at this distance was 32(15) ps. It would seem reasonable to assume that this represents the true lifetime, since the only observed feeding transition (321 keV) was taken into account in the analysis. The long lifetime of the 5^+_1 state results in the low energy tail on the slow component of the 403 keV γ-ray – see Fig. 2. Assuming a pure M1 decay, a feature consistent with the published directional correlation from oriented state (DCO) measurements [24] for the 403 keV γ-ray, the lifetime yields a B(M1;$3^+_1 \rightarrow 2^+_1$) of 0.027(13) μ_N^2. For ^{70}Se, the effective mean lifetimes of all three observed states feeding the yrast 2^+ state were extracted in this work (see Table 1). Typically, delaying effects from higher-lying states result in extracted effective lifetimes that can be longer than the true lifetimes. This was found to be the case for the 4^+_1 and 2^+_2 states in ^{70}Se, where the target-only spectrum shows evidence for known transitions feeding these states. The analysis of the $3^{(-)}_1$ feeding state resulted in a much shorter lifetime than that quoted in the literature. We note, however, this comes from old data [21] which has since been shown to have suspect lifetimes [13].

The simulated fits used to extract the yrast 2^+ state lifetime in ^{70}Br, following corrections for feeding, are shown in Fig. 3. The deduced mean lifetime using a χ^2 fit is $\tau(2^+_1) = 3.96(58)$ ps, which results in a B(E2; $2^+_1 \rightarrow 0^+_{gs}$) of 291(43) e^2 fm^4 – see Table 1. Fig. 4 shows simulated fits used to extract the yrast 2^+ state lifetime in ^{70}Se, following corrections for feeding. The resulting mean lifetime is $\tau(2^+_1) = 3.28(37)$ ps and the corresponding B(E2; $2^+_1 \rightarrow 0^+_{gs}$) of 332(37) e^2 fm^4 is in excellent agreement with the literature value of 342(19) e^2 fm^4 [13]. The lifetime of the first 2^+ state in ^{68}Se was extracted via two methods (a) assuming fast feeding and (b) assuming that the 4^+_1 state lifetime follows the rotational model estimate. The deduced lifetime under the first of these conditions is $\tau(2^+_1) = 4.60(82)$ ps, and is the value given in Table 1. The corresponding B(E2; $2^+_1 \rightarrow 0^+_{gs}$) of 392(70) e^2 fm^4 is in excellent agreement with the literature value of 432(58) e^2 fm^4 [7], suggesting the assumption made regarding the short lifetime of the 4^+_1 state is valid. If one assumes a 4^+_1 state lifetime based on the rotational model estimate with a measured feeding intensity of 48%, the lifetime of the 2^+_1 state reduces to ∼4 ps, which lies within 1σ of the uncorrected value and yields a corresponding B(E2; $2^+_1 \rightarrow 0^+_{gs}$) of ∼450 e^2 fm^4, which remains in very good agreement with the literature value.

The errors quoted for all results in Table 1 include both statistical uncertainties and systematic errors, the latter arising from uncertainties in degrader excitation fraction, foil separation, feeding

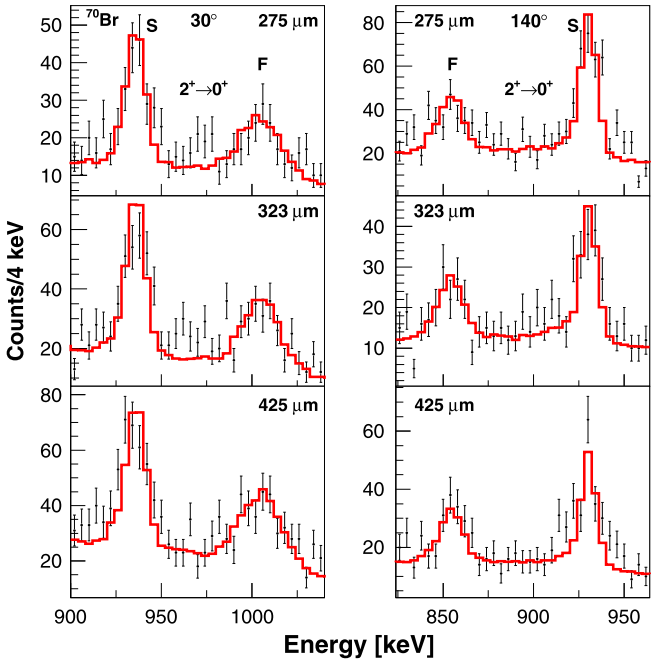

Fig. 3. (Colour online.) Experimental data (black points) and best-fit simulated lineshapes (red line) for the 934 keV $2_1^+ \rightarrow 0_{gs}^+$ transition in ^{70}Br at 30° (left) and 140° (right) detector angles. Fast (F) and slow (S) components are labelled and correspond to decays before and after the degrader foil, respectively. Note that the simulated fit to 140° 425 μm data was not included in the analysis, as the unconventional experimental lineshape resulted in unreliable results.

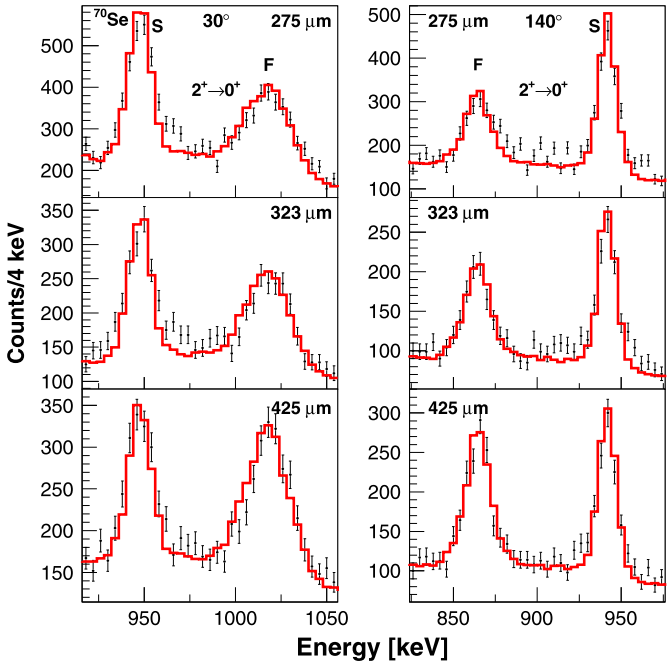

Fig. 4. (Colour online.) Experimental data (black points) and best-fit simulated lineshapes (red line) for the 945 keV $2_1^+ \rightarrow 0_{gs}^+$ transition in ^{70}Se at 30° (left) and 140° (right) detector angles. Fast (F) and slow (S) components are labelled and correspond to decays before and after the degrader foil, respectively.

transition intensity and feeding state lifetime. The largest contributions to the systematic error were from the uncertainties in degrader excitation fraction and foil separation.

It was assumed that the γ-ray angular distributions of all depopulating transitions were isotropic. However, in the case of single/two-nucleon knockout, it is possible that some alignment of

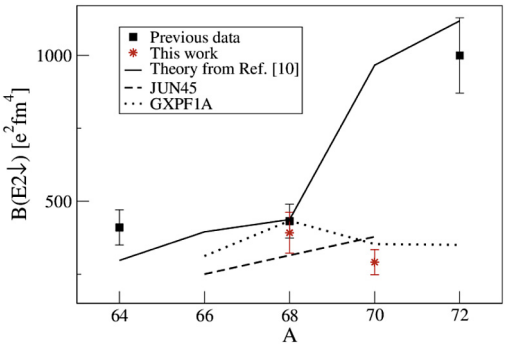

Fig. 5. (Colour online.) Experimental values of $B(E2; 2_1^+ \rightarrow 0_{gs}^+)$ for N = Z nuclei [6–8] (black squares) compared to calculations developed by P. Möller et al. [10] (solid line). Also shown are large-scale shell model calculations using the JUN45 interaction in the $f_{\frac{5}{2}} p g_{\frac{9}{2}}$ model space (dashed line) and using the GXPF1A interaction in the *fp* model space (dotted line). The results obtained in this work are shown by red stars.

Table 2
Large-scale shell model calculations [29–32] of reduced transition strengths for two different interactions. Coulomb, spin-orbit and INC components are included. The JUN45 interaction was utilised with the $f_{\frac{5}{2}} p g_{\frac{9}{2}}$ model space, and the GXPF1A interaction was utilised with the *fp* model space. Also included are present experimental values. B(E2) values are given in units of e^2 fm^4, and B(M1) in units of μ_N^2.

	$B(ML; J_i^\pi \rightarrow J_f^\pi)$	JUN45	GXPF1A	Present
^{70}Br	$B(E2; 5_1^+ \rightarrow 3_1^+)$	195	460	450(110)
^{70}Br	$B(M1; 3_1^+ \rightarrow 2_1^+)$	0.132	0.012	0.027(13)
^{70}Br	$B(E2; 2_1^+ \rightarrow 0_{gs}^+)$	378	353	291(43)
^{70}Se	$B(E2; 2_1^+ \rightarrow 0_{gs}^+)$	348	365	332(37)
^{68}Se	$B(E2; 2_1^+ \rightarrow 0_{gs}^+)$	315	433	392(70)

the outgoing recoils occurs, leading to different γ-ray distributions for dipole and quadrupole transitions [25]. Effects of a 20% alignment (typical for one-nucleon knockout [26]) for the $3_1^+ \rightarrow 2_1^+$ decay on the 2_1^+ lifetime in ^{70}Br were investigated in this work, however this error is not included in the final result in Table 1. Assuming an alignment of 20% for the recoils results in an effective increase of the 403 keV γ-ray intensity from 23.6% to 27.5%, which in turn decreases the lifetime of the 2_1^+ state by 0.06 ps from the value quoted in Table 1 to 3.90 ps ($B(E2\downarrow) = 296$ e^2 fm^4). This effect is small compared to other systematic errors considered in this work.

Fig. 5 shows $B(E2; 2_1^+ \rightarrow 0_{gs}^+)$ values for a range of N = Z nuclei in the A ∼ 70 region (black squares). Included on this plot are the present results obtained for ^{68}Se and ^{70}Br (red stars). The value for ^{70}Br suggests a decrease in collectivity compared to the neighbouring lower mass N = Z nucleus ^{68}Se, which indicates the transition to higher collectivity begins at ^{72}Kr rather than at ^{70}Br. The $B(E2\downarrow)$ systematics for N = Z nuclei shown in Fig. 5 are compared to predictions based on the finite-range droplet macroscopic model and the folded Yukawa single-particle microscopic model [10] (solid line). $B(E2\downarrow)$ values from this model were calculated from deformation parameters by assuming a rigid rotor model. These calculations reproduce the overall trend well, but predict a sharp increase in collectivity at ^{70}Br, which is not supported by the present experimental results.

Table 2 and Fig. 5 compare the present data with our shell model calculations, performed using the GXPF1A interaction [27] in the *fp* model space (including the $f_{\frac{7}{2}}$ orbit) and the JUN45 interaction [28] in the $f_{\frac{5}{2}} p g_{\frac{9}{2}}$ model space (no $f_{\frac{7}{2}}$ orbit). Coulomb, spin-orbit and isospin non-conserving (INC) interactions were included in the calculations, further details of which can be found in Refs. [29–31]. Parameters for the INC interaction were taken

from [32] for the *fp* model space and from [29] for the $f_{\frac{5}{2}}pg_{\frac{9}{2}}$ model space. Standard effective charges of 1.5**e** and 0.5**e** were used for protons and neutrons, respectively. The calculations performed with the GXPF1A interaction and the *fp* model space yield the best agreement with the B(E2↓) values deduced for ^{68}Se and ^{70}Br, both in terms of trend and absolute values. Calculations using the JUN45 interaction in an $f_{\frac{5}{2}}pg_{\frac{9}{2}}$ model space fail to replicate the decrease in collectivity in ^{70}Br relative to ^{68}Se. The level of agreement between the data and the GXPF1A calculations suggests the $g_{\frac{9}{2}}$ orbital is not important for describing the low-lying states in ^{68}Se and ^{70}Br. However, it would be significant for ^{72}Kr because the calculated B(E2↓) value, using this interaction, of 350 $e^2\,fm^4$ cannot reproduce the rapid enhancement at A = 72 seen in Fig. 5. All calculations were repeated without the INC interaction. This resulted in no significant change to the predicted B(E2) values with either interaction.

The B(E2) values for ^{68}Se and ^{70}Br tentatively suggest a staggering between even–even and odd–odd N = Z nuclei in this region. Since the current work provides the first measurement of a 2_1^+ state lifetime in an odd–odd N = Z nucleus around A ∼ 70, it is not yet clear if this is a significant feature. Measurements of other neighbouring odd–odd nuclei such as ^{66}As and ^{74}Rb will be important in establishing whether staggering of the B(E2:$2_1^+ \rightarrow 0_{gs}^+$) values between even–even and odd–odd N = Z nuclei is a regular feature in this region.

From a theoretical perspective, it is possible that the staggering pattern results from the presence of two T = 0 monopole attractions between the $\pi f_{\frac{7}{2}}$, $\nu f_{\frac{5}{2}}$ and $\pi p_{\frac{3}{2}}$, $\nu p_{\frac{1}{2}}$ orbitals, respectively. The monopole attractions between these are stronger than those of other monopole matrix elements (see [27]). This results in nucleons being more easily excited from the $f_{\frac{7}{2}}p_{\frac{3}{2}}$ to the $f_{\frac{5}{2}}$, and yields an increase in the B(E2) value at A = 68 as seen in Fig. 5. Furthermore, the region where staggering is observed may be limited since in the lower mass region the $\nu f_{\frac{5}{2}}$ and $\nu p_{\frac{1}{2}}$ occupations will be small, whilst in the A ∼ 80 region the $g_{\frac{9}{2}}$ orbit plays a key role.

The small B(M1) value deduced for the $3_1^+ \rightarrow 2_1^+$ decay in ^{70}Br is interesting. B(M1) values resulting from ΔT = 1 transitions in odd–odd N = Z nuclei have been discussed in terms of the quasideuteron picture of valence nucleons [33]. It can be shown that M1 transition strengths can be derived using a single-j approximation, with the possibility of two cases: the quasideuteron case, where the orbital and spin terms of valence nucleons add together and lead to an increased B(M1) ($j = \ell + \frac{1}{2}$); and the non-quasideuteron case, where there is a cancellation of the spin and orbital terms and a correspondingly hindered B(M1) ($j = \ell - \frac{1}{2}$). Both cases are seen in the literature across the nuclide chart (see Ref. [33] and references therein). Whilst discussions in Ref. [33] focus on $1^+ \rightarrow 0^+$ transitions, the measurement of the 3_1^+ lifetime in ^{70}Br is interesting because $3^+ \rightarrow 2^+$ transitions serve as an analogue. It is assumed the J = 2 core configuration does not mix with the valence nucleons. The small B(M1) value obtained for the $3_1^+ \rightarrow 2_1^+$ decay in ^{70}Br is indicative of the non-quasideuteron scenario, suggesting the main component of the 3_1^+ wavefunction should involve the odd proton and neutron primarily occupying $f_{\frac{5}{2}}$ orbitals.

The hindered nature of the B(M1) is consistent with our shell model calculations using the GXPF1A interaction in an *fp* model space, which predict a small B(M1) value for the $3_1^+ \rightarrow 2_1^+$ transition in ^{70}Br (see Table 2). It was found that the inclusion of the $f_{\frac{7}{2}}$ orbit was essential to replicate the experimental B(M1) value. The GXPF1A calculations, which give a multipole mixing ratio for the $3_1^+ \rightarrow 2_1^+$ transition of $\delta(E2/M1) \simeq 0.02$, are in agreement with our assumption of a pure dipole nature for this transition.

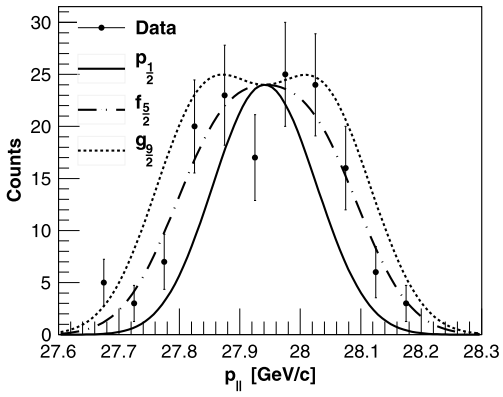

Fig. 6. Experimental momentum distribution of ^{70}Br recoils from target-only data gated on the $3_1^+ \rightarrow 2_1^+$ transition with background subtraction (data points). The solid, dot-dashed and dotted lines show calculated recoil momentum distributions assuming the knocked-out neutron in ^{71}Br resides in the $p_{\frac{3}{2}}$, $f_{\frac{5}{2}}$ and $g_{\frac{9}{2}}$ single particle orbital, respectively [34]. The calculations have been adjusted to account for target broadening effects.

Fig. 6 shows the experimental momentum distribution of ^{70}Br recoils after gating target-only data on the $3_1^+ \rightarrow 2_1^+$ transition with a background subtraction, compared to various calculated momentum distributions based on the eikonal reaction theory [34]. Background contributions were removed by subtracting a momentum distribution gated on a γ background close in energy to the $3_1^+ \rightarrow 2_1^+$ transition peak and with an identical width (in bins) to the gate for the 403 keV γ-ray. The solid, dot-dashed and dotted theoretical distributions in Fig. 6 correspond to calculations assuming the knocked-out neutron in ^{71}Br resides in the $p_{\frac{3}{2}}$, $f_{\frac{5}{2}}$ and $g_{\frac{9}{2}}$ orbital, respectively. The experimental distribution, which includes feeding to the 3_1^+ state as well as direct population, appears most consistent with the removal of an $\ell = 3$ ($f_{\frac{5}{2}}$) orbit nucleon. This result suggests an f-wave dominance in the configuration of low-lying excited states in ^{70}Br, and is therefore consistent with the information deduced from the B(M1) value for the $3_1^+ \rightarrow 2_1^+$ transition.

A comparison of 2_1^+ state lifetimes in ^{70}Br and ^{70}Se is interesting in view of previous discussions on potential differences in analogue state shapes in A ∼ 70 nuclei at low spin [11,35–37]. The deduced B(E2) values in this work for the $2_1^+ \rightarrow 0_{gs}^+$ decays indicate the two nuclei have similar structures at low spin. Our shell model calculations using the GXPF1A interaction in an *fp* model space result in calculated values of the B(E2; $2_1^+ \rightarrow 0_{gs}^+$) for ^{70}Br(^{70}Se) of 353(365) $e^2\,fm^4$, which also suggest similar levels of collectivity in the two nuclei, in reasonable agreement with what is experimentally observed – see Table 2. The GXPF1A interaction predicts the B(E2) value in ^{70}Se is slightly higher than in ^{70}Br, but this situation is reversed for calculations performed with the JUN45 interaction. More precise B(E2) values will be required to provide a better test of these differences. Excluding the INC interaction in the shell model calculations with either the GXPF1A or JUN45 interaction was found to have a negligible effect on the calculated B(E2) values.

In summary, the recoil distance Doppler shift technique was used in combination with nucleon knockout and inelastic scattering reactions to obtain lifetime measurements of the T = 1 2_1^+ state in ^{70}Se; the T = 1 2_1^+ state and T = 0 3_1^+, 5_1^+ states in ^{70}Br; and the T = 0 2_1^+ state in ^{68}Se. The ^{70}Br 2_1^+ state lifetime result suggests slightly reduced collectivity in this nucleus compared to that of its lower mass N = Z neighbour ^{68}Se, a feature that can be reproduced by shell model calculations using the GXPF1A inter-

action and the *fp* model space. The result for the 2_1^+ state lifetime in ^{68}Se yields a B(E2↓) value that is consistent with the B(E2↑) obtained from relativistic Coulomb excitation measurements. There is evidence for a staggering of the B(E2) values between the even–even and odd–odd N = Z nuclei between mass 68 and 72, but data in other odd–odd N = Z nuclei are required to confirm if this is a trend in the region. The lifetime of the first excited 2^+ state in ^{70}Se was found to agree with previous work. The level of collectivity for the $2_1^+ \rightarrow 0_{gs}^+$ transitions in ^{70}Br and ^{70}Se, given by the B(E2) values, is found to be very similar, suggesting there is no major shape change between the two nuclei at low spin, which is consistent with what is expected for analogue states. The results can be nicely reproduced by shell model calculations in an *fp* model space, where the $f_{\frac{7}{2}}$ orbital appears to play an important role. All experimental results in this work are consistent with a lack of any significant $g_{\frac{9}{2}}$ orbital occupation in the low-lying excited states of A ∼ 70, N = Z nuclei up to and including ^{70}Br.

Acknowledgements

This work is supported by the National Science Foundation (NSF) under PHY-1102511, the Department of Energy (DOE) National Nuclear Security Administration under Award Number DE-NA0000979 and Contract Number DE-FG02-96ER40983, BMBF (Germany) under Contract Number 05P12PKFNE, and the UK STFC under Grant Number ST/J000124/1.

References

[1] A.O. Macchiavelli, et al., Phys. Rev. C 61 (2000) 041303(R).
[2] M. Hasagawa, et al., Phys. Lett. B 656 (2007) 51.
[3] W. Nazarewicz, et al., Nucl. Phys. A 435 (1985) 397.
[4] Y. Fu, et al., Phys. Rev. C 87 (2013) 054305.
[5] M. Bender, et al., Phys. Rev. C 74 (2006) 024312.
[6] K. Starosta, et al., Phys. Rev. Lett. 99 (2007) 042503.
[7] A. Obertelli, et al., Phys. Rev. C 80 (2009) 031304(R).
[8] A. Gade, et al., Phys. Rev. Lett. 95 (2005) 022502.
[9] A. Lemasson, et al., Phys. Rev. C 85 (2012) 041303(R).
[10] P. Möller, et al., At. Data Nucl. Data Tables 59 (1995) 185–381.
[11] G. de Angelis, et al., Phys. Rev. C 85 (2012) 034320.
[12] A. Petrovici, et al., J. Phys. G 32 (2006) 583–597.
[13] J. Ljungvall, et al., Phys. Rev. Lett. 100 (2008) 102502.
[14] P. Miller, et al., in: Proceedings of the 2001 Particle Accelerator Conference, Chicago, IL, IEEE, Piscataway, NJ, 2001, p. 2557.
[15] D.J. Morrisey, et al., Nucl. Instrum. Methods Phys. Res. Sect. B 204 (2003) 90.
[16] D. Bazin, et al., Nucl. Instrum. Methods Phys. Res. Sect. B 204 (2003) 629.
[17] A. Dewald, et al., in preparation.
[18] A. Dewald, et al., Prog. Part. Nucl. Phys. 67 (2012) 786.
[19] B. Pritychenko, et al., At. Data Nucl. Data Tables 98 (2012) 798–811.
[20] W.F. Mueller, et al., Nucl. Instrum. Methods Phys. Res. Sect. A 466 (2001) 492–498.
[21] J. Heese, et al., Z. Phys. A 325 (1986) 43–53.
[22] S. Agostinelli, et al., Nucl. Instrum. Methods Phys. Res. Sect. A 598 (2003) 250–303.
[23] P. Adrich, et al., Nucl. Instrum. Methods Phys. Res. Sect. A 598 (2009) 454.
[24] D.G. Jenkins, et al., Phys. Rev. C 65 (2002) 064307.
[25] K.S. Krane, et al., At. Data Nucl. Data Tables 11 (1973) 351–406.
[26] H. Olliver, et al., Phys. Rev. C 68 (2003) 044312.
[27] M. Honma, et al., Phys. Rev. C 69 (2004) 034335.
[28] M. Honma, et al., Phys. Rev. C 80 (2009) 064323.
[29] K. Kaneko, et al., Phys. Rev. C 82 (2010) 061301.
[30] K. Kaneko, et al., Phys. Rev. Lett. 109 (2012) 092504.
[31] K. Kaneko, et al., Phys. Rev. C 89 (2014) 031302(R).
[32] A.P. Zuker, et al., Phys. Rev. Lett. 89 (2002) 142502.
[33] A.F. Lisetskiy, et al., Phys. Rev. C 60 (1999) 064310.
[34] P.G. Hansen, J.A. Tostevin, Annu. Rev. Nucl. Part. Sci. 53 (2003) 219–261.
[35] B.S. Nara Singh, et al., Phys. Rev. C 75 (2007) 061301(R).
[36] M.A. Bentley, S.M. Lenzi, Prog. Part. Nucl. Phys. 59 (2007) 497–561.
[37] A. Petrovici, et al., Nucl. Phys. A 605 (1996) 290.